

Computing expectation values of density matrices for quantum anomaly detection

Diego H. Useche, Oscar A. Bustos-Brinez, Joseph A. Gallego,
Fabio A. González

MindLab Research Group, Universidad Nacional de Colombia, Bogotá, Colombia

E-mail: {diusecher, oabustosb, jagallegom, fagonzalezo}@unal.edu.co

January 2022

Abstract.

This article presents a novel classical-quantum anomaly detection model based on density estimation and the expected values of density matrices. The core subroutine of the proposed method is a qubit-based quantum protocol whose task is to compute the expected value of a density matrix, being flexible enough to support the use of pure and mixed states approaches. The anomaly detection model is tested with pure and mixed states on a synthetic data set for density estimation and on a widely used real-life data set for anomaly detection; results show higher accuracy with mixed states for both tasks.

1. Introduction

A problem of interest in many areas of science and engineering is anomaly detection (AD). This problem aims to determine which samples from a given data set are “ordinary” or “normal” (being the definition of “normal” defined by each particular case) and which samples depart or are deviated from “normal” data (commonly known as “anomalies” or “outliers”). Some common applications of anomaly detection include fraud detection [1] and medical diagnosis [2]. Many classical algorithms have been proposed to detect such anomalies [3, 4]; however, recent works have shown some advantages of combining quantum computation with AD tasks. For instance, some of the quantum versions of the ADDE algorithm (Algorithm Detection Based on Density Estimation) [5], the kernel principal component analysis and the one-class support vector machine [6] utilize less resources and present exponential speed-ups in contrast to their classical counterparts.

A well known approach to perform AD is density estimation (DE). This method consists of estimating a probability density function (pdf) of normal data and classifying as anomalies new samples which lie below a certain probability threshold. Some classical techniques include the ADDE [7] mentioned before, and the SmartSifter method, which uses a finite mixture model [8]. Some quantum algorithms include the quantum ADDE

which operates with amplitude estimation [5], and a quantum clustering method which exploits the variations in the density function to detect anomalies [9].

In this article, we propose a hybrid classical-quantum anomaly detection method, which extracts probability density functions of both “normal” and “anomalous” data, and classifies new samples as “normal” or “anomalies” if they lie either above or below a certain probability threshold. Our method implements the prediction phase of a quantum-inspired density estimation algorithm called the Density Matrix Kernel Density Estimation (DMKDE) proposed by Gonzalez et. al. [10]. In this paper we extend to qubits a previous implementation of the DMKDE on a qudit-based quantum computer [11].

One of the main results of the article is the statement of a quantum protocol to estimate the expected value of a density matrix in a quantum computer which operates on qubits, through a quantum circuit used to implement the prediction phase of the DMKDE. In contrast to methods like Quantum State Tomography [12, 13, 14] or Variational Quantum Eigensolver [15], which estimate and codify a density matrix in terms of the Pauli matrices, our quantum algorithm computes the expected value of a density matrix given its spectral decomposition.

The outline of the article is as follows: In Sect. 2 we present the theoretical background of the DMKDE algorithm, the notation of the quantum circuits, and a previously proposed quantum protocol [16] to compute the expected value of a density matrix of a pure state, in Sect. 3, we introduce our proposed quantum anomaly detection method, and outline the proposed quantum circuit to estimate the expected value of a mixed state density matrix. In Sect. 4, we illustrate the results of our proposed method for density estimation and anomaly detection, and finally we establish our conclusions and future research in Sect. 5.

2. Preliminaries

In this section, we present the DMKDE algorithm proposed by Gonzalez et al. [10], which is a non-parametric density estimation method based on density matrices and random features [17]. In particular, we describe two approaches of the method: pure and mixed states. Additionally, we explain the notation of the quantum circuits used through the article, and present a previous work [16] to compute the expected value of a pure state density matrix in quantum computer.

2.1. Density Matrix Kernel Density Estimation

The machine learning algorithm Density Matrix Kernel Density Estimation (DMKDE) [10] constructs a density matrix of the training data and estimates the probability of a testing sample by computing the expected value of the testing state with the training density matrix.

The method starts by applying a quantum feature map, based on Random Fourier

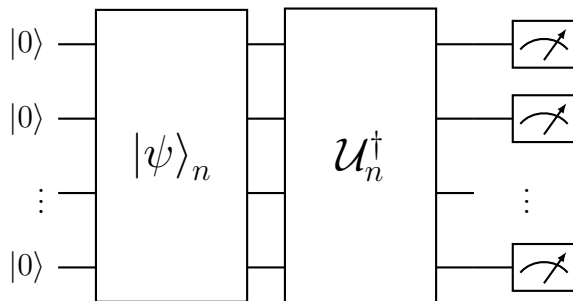


Figure 1. DMKDE quantum circuit for pure states [16].

Features (RFF) [17, 18], to each sample in the train and test data set $x \rightarrow |\psi\rangle$, where $\psi \in \mathbb{C}^d$ and $\langle\psi|\psi\rangle = 1$. The RFF create a quantum embedding whose inner product approximates a similarity measure of the classical data; this measure is the Radial Basis Function (RBF) kernel. The parameters of RFF are the inverse of the standard deviation of the RBF, denoted as γ (gamma), and the dimension of the quantum features d .

The DMKDE method explores two approaches to train the density matrix, pure and mixed states. For the training states $|\psi_i\rangle$ for $i \in \{0, 1, \dots, N-1\}$, the pure state density matrix is computed by,

$$|\phi_{\text{train},1}\rangle = \frac{\sum_i |\psi_i\rangle}{\|\sum_i |\psi_i\rangle\|}, \quad \text{and} \quad \rho_{\text{train},1} = |\phi_{\text{train},1}\rangle \langle\phi_{\text{train},1}|, \quad (1)$$

and, for the mixed state by,

$$\rho_{\text{train},2} = \frac{1}{N} \sum_{i=0}^{N-1} |\psi_i\rangle \langle\psi_i|, \quad (2)$$

the indices 1 and 2 refer to the pure and mixed approaches respectively. The probability estimators of a new test sample $|\psi\rangle$ can be computed by,

$$\hat{p}_1(|\psi\rangle) = C_{\gamma,1} \sqrt{\langle\psi|\rho_{\text{train},1}|\psi\rangle} = C_{\gamma,1} \sqrt{\langle\phi_{\text{train},1}|\psi\rangle^2}, \quad (3)$$

$$\hat{p}_2(|\psi\rangle) = C_{\gamma,2} \langle\psi|\rho_{\text{train},2}|\psi\rangle, \quad (4)$$

where $C_{\gamma,1}$ and $C_{\gamma,2}$ are normalization constants that depend on the parameter γ .

The DMKDE algorithm is an efficient approximation of the Parzen–Rosenblatt window [19, 20], a non-parametric method for density estimation.

2.2. Notation and DMKDE quantum circuit for pure states

We now introduce the notation of the quantum circuits used through the article, which is the same notation used in [21]. Any state of the canonical basis of a n -qubit state can be written as $|b_0 b_1 \dots b_{n-1}\rangle$ with $b_i \in \{0, 1\}$, hence, we may write any state in the

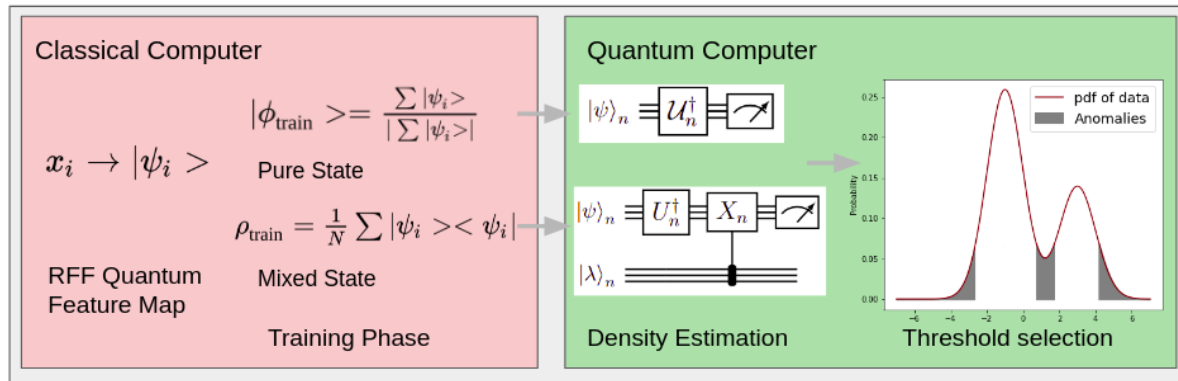


Figure 2. Classical-quantum anomaly detection model.

canonical basis as a string in its binary form. This notation can be simplified by writing such state as $|\sum_{i=0}^{n-1} b_i 2^i\rangle_n$, namely, the bit-string is written in decimal form and the subindex indicates the number of qubits of the state. For example, the 4-qubit state $|1010\rangle$ can be written as $|5\rangle_4$. We make use of the same subindex to illustrate the number of qubits in which a unitary gate or a quantum state initialization act upon.

Once established the circuits notation, we present a previously proposed quantum technique [16] to compute the expected value of a pure state density matrix, which is equivalent to calculate the inner product of two quantum states, as indicated by Eq. 3.

The circuit starts by initializing a n -qubit state with the state $|\psi\rangle_n \in \mathbb{C}^d$, with $2^{n-1} < d \leq 2^n$, by means of amplitude encoding [22], and then it applies to the n qubits a unitary matrix \mathcal{U}_n^\dagger , which satisfies that $\mathcal{U}_n |0\rangle_n = |\phi_{\text{train},1}\rangle$, see Eq. 1 and Figure 1. By measuring the n qubits, the probability of the state $|0\rangle_n$ is the expected value of a pure state density matrix. In this article, we present a more general quantum protocol to estimate the expected value a mixed state density matrix in a qubit-based quantum computer.

3. Quantum anomaly detection method

We propose a hybrid classical-quantum model for anomaly detection based on the DMKDE algorithm [10] for both pure and mixed states. The steps of the method are: (i) quantum feature map, (ii) training phase, (iii) density estimation of new samples, and (iv) threshold selection and classification. The steps (i), (ii) and (iv) were calculated in a classical computer, while the step (iii) was computed in a quantum computer simulator. These steps are explained in more detail below.

- (i) Quantum feature map: Given a dataset to classify, split it into three partitions: train, validation and test, in such a way that each of them is composed of both “normal” and “outlier” data. Then apply a quantum feature map $x_i \rightarrow |\psi_i\rangle$ based on Random Fourier Features, or RFF [17, 18] to all of these partitions.
- (ii) Training phase: Use the training data to compute either the training quantum

state $|\phi_{\text{train},1}\rangle$ for the pure state or the training density matrix $\rho_{\text{train},2}$ for the mixed state, see Equations 1 and 2. When using mixed state approach, also calculate the spectral decomposition of the training density matrix $\rho_{\text{train},2} = V\Lambda V^\dagger$. The training pure and mixed quantum states encode probability distributions of the train dataset.

- (iii) Density estimation of new samples: Estimate the probability density values of the validation and test partitions by computing the probability estimation of the samples with the training density matrix. The estimator of the pure state (see Eq. 3) is obtained using the quantum circuit shown in Figure 1 [16]. To calculate the probability estimator of a mixed state (see Equation 4), use the proposed quantum circuit shown in Figure 3. See Sect. 3.1 for the mathematical details of the mixed state quantum circuit.
- (iv) Threshold selection: Once given the probability estimations, use the validation dataset to select a threshold to differentiate the samples: if a sample has a density lower than the threshold, then it is considered as an “outlier”. Since the validation samples are both normal data and outliers, the threshold must be somewhere between the maximum and minimum density values. A percentile is set to discriminate between normal and anomalous validation samples, but other metrics can be used. Finally, use this threshold to classify the samples in test partition.

Next, we present the theoretical development of the proposed quantum protocol to compute the expected value of a mixed state density matrix. The following section explains the proposed implementation of the prediction phase of the DMKDE method for mixed states.

3.1. DMKDE quantum circuit for mixed states

In order to simulate the prediction phase of the DMKDE, see Eq. 4, we propose a novel quantum protocol to estimate the expected value of a mixed state density matrix in a qubit-based quantum computer. This circuit expands to qubits a previous implementation of the mixed state DMKDE in a high-dimensional quantum computer [11].

We want to compute the expected value of a density matrix $\rho \in \mathbb{C}^{d \times d}$ with a quantum state $|\psi\rangle \in \mathbb{C}^d$ in a quantum computer. This calculation requires $2 \times n$ qubits, with $2^{n-1} < d \leq 2^n$. The first n qubits encode the state $|\psi\rangle$ and the unitary matrix V^\dagger whose rows are the complex conjugate eigenvectors of ρ , and the remaining n qubits encode the eigenvalues of the density matrix.

To begin with, as noted in [11], we have that,

$$\langle \psi | \rho | \psi \rangle = \langle \psi | V \left(\sum_{i=0}^{d-1} \lambda_i |i\rangle \langle i| \right) V^\dagger | \psi \rangle = \sum_{i=0}^{d-1} \lambda_i \left| \langle i | V^\dagger | \psi \rangle \right|^2, \quad (5)$$

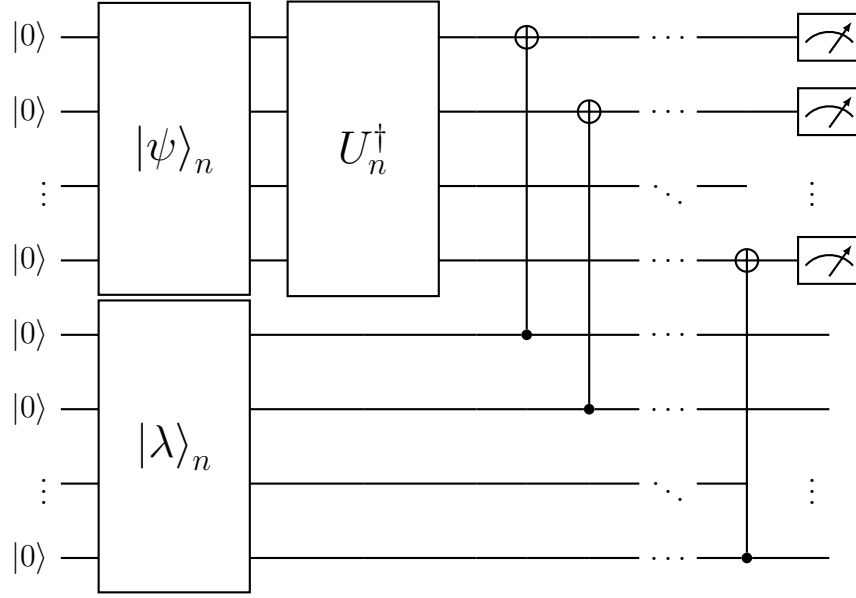


Figure 3. DMKDE quantum circuit for mixed states.

where, $V \in \mathbb{C}^{d \times d}$ is the unitary matrix of eigenvectors and $\Lambda = \sum_{i=0}^{d-1} \lambda_i |i\rangle \langle i|$ is the diagonal matrix of eigenvalues.

The proposed DMKDE quantum circuit starts by initializing the first n qubits with the state $|\psi\rangle_n$, see the notation in Sect. 2.2, and the remaining n qubits with the state $|\lambda\rangle_n = \sum_{i=0}^{d-1} \sqrt{\lambda_i} |i\rangle_n$, state that encodes the eigenvalues of ρ , see Fig. 3. This operation can be performed thanks to amplitude encoding [22]. We have that,

$$|\psi\rangle_n \otimes |\lambda\rangle_n = |\psi\rangle_n \otimes \sum_{i=0}^{d-1} \sqrt{\lambda_i} |i\rangle_n. \quad (6)$$

Next, we construct a unitary matrix U_n^\dagger see Eq. 7, whose first quadrant is composed of the unitary matrix V^\dagger and its fourth quadrant with the identity matrix $I_{2^{n-d}}$,

$$U_n^\dagger = \left(\begin{array}{c|c} V^\dagger & \\ \hline & I_{2^{n-d}} \end{array} \right), \quad (7)$$

this unitary matrix U_n^\dagger is applied to the first n qubits in the form of an isometry [21]. We would have,

$$U_n^\dagger |\psi\rangle_n \otimes \sum_{i=0}^{d-1} \sqrt{\lambda_i} |i\rangle_n. \quad (8)$$

We can write the state of the first n qubits as, $U_n^\dagger |\psi\rangle_n = \sum_{i=0}^{d-1} a_i |i\rangle_n$. Where,

$$\|a_i\|^2 = \|\langle i|_n U_n^\dagger |\psi\rangle_n\|^2 = \|\langle i| V^\dagger |\psi\rangle\|^2, \quad (9)$$

namely, $\|a_i\|^2$ is the probability to measure $U_n^\dagger |\psi\rangle_n$ in the canonical state $|i\rangle_n$. Therefore, the circuit leads,

$$\begin{aligned} U_n^\dagger |\psi\rangle_n \otimes |\lambda\rangle_n &= \sum_{i=0}^{d-1} a_i |i\rangle_n \otimes \sum_{j=0}^{d-1} \sqrt{\lambda_j} |j\rangle_n \\ &= \sum_{i=0}^{d-1} a_i \sqrt{\lambda_i} |i\rangle_n \otimes |i\rangle_n + \sum_{\{(i,j):i \neq j\}} a_i \sqrt{\lambda_j} |i\rangle_n \otimes |j\rangle_n. \end{aligned}$$

We then apply a series of n CNOT gates, between the first and the second halves of the circuit, as shown in Fig. 3. The i^{th} CNOT operates with control the $(i+n)^{\text{th}}$ qubit and target the i^{th} qubit, with $i \in \{0, \dots, n-1\}$. The effect of this series of CNOT gates can be observed by writing,

$$|i\rangle_n \otimes |j\rangle_n = \left| \sum_{k=0}^{n-1} b_k^i 2^k \right\rangle_n \otimes \left| \sum_{l=0}^{n-1} b_l^j 2^l \right\rangle_n, \quad (10)$$

where, $|b_0^i b_1^i \dots b_{n-1}^i\rangle$ and $|b_0^j b_1^j \dots b_{n-1}^j\rangle$ are the binary representations of $|i\rangle_n$ and $|j\rangle_n$ respectively. The n CNOT gates have the same complexity as a single CNOT, as they can be parallelized in a quantum computer [23].

We represent this series of n CNOT gates with the $2n$ -qubit unitary operation U_{2n}^{Cnot} . The outcome of this transformation is a qubit-wise summation modulo 2 (denoted with \oplus) on the first half of the circuit,

$$U_{2n}^{\text{Cnot}}(|i\rangle_n \otimes |j\rangle_n) = \left| \sum_{k=0}^{n-1} (b_k^i \oplus b_k^j) 2^k \right\rangle_n \otimes \left| \sum_{l=0}^{n-1} b_l^j 2^l \right\rangle_n. \quad (11)$$

If $i = j$ we would have that,

$$U_{2n}^{\text{Cnot}}(|i\rangle_n \otimes |i\rangle_n) = |0\rangle_n \otimes \left| \sum_{l=0}^{n-1} b_l^i 2^l \right\rangle_n \quad (12)$$

In contrast, if $i \neq j$, the resulting state, $\left| \sum_k (b_k^i \oplus b_k^j) 2^k \right\rangle_n$, would be distinct to the $|0\rangle_n$ state.

Therefore, after applying the series of n CNOT gates, the DMKDE quantum circuit leads to,

$$\sum_{i=0}^{d-1} a_i \sqrt{\lambda_i} |0\rangle_n \otimes |i\rangle_n + \sum_{\{(i,j):i \neq j\}} a_i \sqrt{\lambda_j} \left| \sum_k (b_k^i \oplus b_k^j) 2^k \right\rangle_n \otimes |j\rangle_n.$$

By measuring the first n qubits the probability of state $|0\rangle_n$ would be,

$$P(|0\rangle_n) = \sum_{i=0}^{d-1} \|a_i\|^2 \lambda_i = \sum_{i=0}^{d-1} \lambda_i \left\| \langle i | V^\dagger |\psi\rangle \right\|^2 = \langle \psi | \rho | \psi \rangle, \quad (13)$$

see Eqs. 5 and 9.

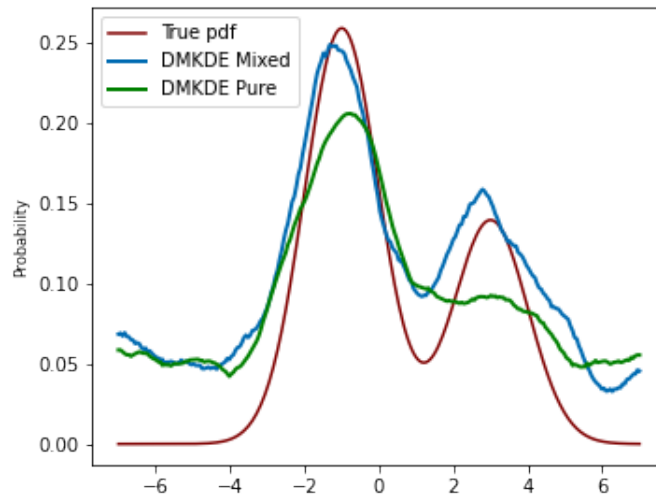


Figure 4. Density estimation pure and mixed states.

4. Results

4.1. Quantum density estimation

As mentioned in Sect. 2, the DMKDE algorithm [10] encodes in a density matrix a probability distribution of training data see Eqs. 1 and 2, and estimates the probability of new testing samples see Eqs. 3 and 4. Therefore, the DMKDE algorithm can approximate a probability density function without optimization.

To test the DMKDE algorithm and the proposed DMKDE quantum circuit for mixed states, see Sect. 3.1, we constructed a 1-Dimensional probability density function made of two interpenetrating gaussians. The training data set was composed of 1000 points sampled from the pdf, and the testing data set was formed by 250 equidistant points. A quantum feature map with 16 RFF with $\gamma = 1$, was applied to both train and test data set, the resulting training density matrix had a dimension of 16x16. We computed the probability estimator for both pure and mixed states, see Eqs. 3 and 4, the pure state estimator was computed with the circuit proposed by Liu et al. [16], and the mixed state estimator with our proposed DMKDE quantum circuit, see Fig. 3. Due to the randomness of the RFF, we did 10 experiments for both pure and mixed states with the Qiskit QASM simulator, averaging the estimations of the density functions. The results are shown in Fig. 4.

The figure shows the averaged density estimation of the test data set for pure and mixed states. In comparison with the pure state, the mixed state creates a better approximation of the pdf, specially, in high-density regions. To improve the estimation of the pdf and reduce the noise on low density regions, it is required a higher number of RFF components and henceforth a bigger density matrix.

4.2. Quantum anomaly detection

Once the ability of the proposed circuits to approximate probability density functions was established, a similar experiment was performed with a real-life, previously labeled dataset. For this purpose, we chose Cardiotocography dataset from the UCI Machine Learning Repository, related to heart diseases. It consists of 2068 samples, where each sample contains 22 attributes, and healthy patients make up the “normal” class. This dataset was divided into three partitions: training (60%), validation (20%) and test (20%), all of which contain both normal samples and outliers in the same proportion (specifically, 20% of all samples were labeled as “outliers”).

As a first step, RFF was applied on the samples of all partitions as a quantum feature map; to evaluate the effect of the number of dimensions on the classification, we worked with 4 and 8 dimensions of RFF (which, once normalized, correspond to quantum states of 2 and 3 qubits, respectively). With the quantum states of the training partition samples, we calculated the density matrices for pure states $\rho_{train,1}$ (see Eq. 1) and for mixed states $\rho_{train,2}$ (see Eq. 2), and then we used them to build the respective quantum circuits. These circuits were then run on the QASM simulator of the IBM-Qiskit platform, performing an iteration of the circuit for each sample in validation and test partitions in order to obtain the density estimate for that sample. After obtaining the density values for all samples, the classification of each one as “normal” or “outlier” requires comparing its density value with a threshold value t . The search for the threshold was performed over the validation partition, by setting a percentile threshold t such that 20% of the samples lay below it, thus being considered as anomalies. We then used the obtained t to classify the test samples.

In [10], the authors highlight the influence of the γ parameter used in RFF mapping over the performance of the classifier algorithm. For this reason, we performed a search for an optimal value of γ , noticing that this optimal value is closely related to the inner structure of the dataset; in all scenarios, we chose the value $\gamma = 1$. We ran each circuit ten times, randomizing the quantum RFF embedding in each iteration.

The metrics of the classifiers for 4 and 8 dimensions of RFF, working with both pure and mixed states, were calculated using functions provided in the Scikit-Learn Python library. Results are presented in Table 1.

Size	Method	Accuracy	F1-Score (macro)
RFF dim: 4	Pure State	0.7311 ± 0.0336	0.5690 ± 0.0431
	Mixed State	0.7313 ± 0.0563	0.5681 ± 0.0882
RFF dim: 8	Pure State	0.7447 ± 0.0434	0.5978 ± 0.0608
	Mixed State	0.7609 ± 0.0506	0.6047 ± 0.0893

Table 1. Obtained metrics for Quantum Anomaly Detection experiments.

5. Conclusions

In this article, we presented a classical-quantum anomaly detection model, based on the Density Matrix Kernel Density Estimation algorithm introduced by Gonzalez et al. [10]. Our proposed AD technique works by estimating a probability density function from “normal” and “anomalous” data and classifying test data as “normal” or “outlier” by setting a probability threshold in the pdf that acts as a boundary between these regions. Furthermore, we proposed the DMKDE quantum protocol, which estimates the expected value of any density matrix in a qubit-based quantum computer. This quantum protocol acts as a subroutine in our AD algorithm.

We explored two approaches within our method to perform the estimations: pure and mixed states. We then applied it for two different objectives, density estimation of a given pdf function and anomaly detection from a real dataset; we evaluated the model with quantum Random Fourier features of 4 and 8 dimensions for anomaly detection, and with 16 dimensions for density estimation. The results indicated a small advantage of the mixed state approach on both cases, which indicates that our method is more flexible and may exhibit better results than previous works based solely on pure states. We noticed generally better metrics with a higher number of RFF, but the reported results indicate that the performance of our method can be further improved.

Future work of the proposed classical-quantum AD technique includes comparing our method with other classical and quantum anomaly detection methods, and increasing the number of random features and hence augmenting the size of the quantum circuits. For the proposed DMKDE quantum circuit, we would like to vindicate that our quantum protocol represents a quantum advantage with respect to classical counterparts, and that it is a feasible approach for near-term quantum computers [24], through studying its sensitivity to quantum noise. An interesting future endeavor involves integrating the proposed DMKDE quantum circuit with variational quantum algorithms to learn mixed quantum states in a quantum computer.

References

- [1] Véronique Van Vlasselaer, Cristián Bravo, Olivier Caelen, Tina Eliassi-Rad, Leman Akoglu, Monique Snoeck, and Bart Baesens. APATE: A novel approach for automated credit card transaction fraud detection using network-based extensions. *Decision Support Systems*, 75:38–48, 7 2015. ISSN 0167-9236. doi: 10.1016/J.DSS.2015.04.013.
- [2] Li Fei Chen. An improved negative selection approach for anomaly detection: with applications in medical diagnosis and quality inspection. *Neural Computing and Applications 2011 22:5*, 22(5):901–910, 12 2011. ISSN 1433-3058. doi: 10.1007/S00521-011-0781-5. URL <https://link.springer.com/article/10.1007/s00521-011-0781-5>.
- [3] Caleb C. Noble and Diane J. Cook. Graph-based anomaly detection. *Proceedings*

- of the ACM SIGKDD International Conference on Knowledge Discovery and Data Mining, pages 631–636, 2003. doi: 10.1145/956750.956831.
- [4] Fabio A. González and Dipankar Dasgupta. Anomaly Detection Using Real-Valued Negative Selection. *Genetic Programming and Evolvable Machines 2003 4:4*, 4 (4):383–403, 12 2003. ISSN 1573-7632. doi: 10.1023/A:1026195112518. URL <https://link.springer.com/article/10.1023/A:1026195112518>.
- [5] Ming-Chao Guo, Hai-Ling Liu, Yong-Mei Li, Wen-Min Li, Su-Juan Qin, Qiao-Yan Wen, and Fei Gao. Quantum algorithms for anomaly detection using amplitude estimation. 9 2021. URL <https://arxiv.org/abs/2109.13820v1>.
- [6] Nana Liu and Patrick Rebentrost. Quantum machine learning for quantum anomaly detection. *Physical Review A*, 97(4):042315, 4 2018. ISSN 24699934. doi: 10.1103/PHYSREVA.97.042315/FIGURES/1/MEDIUM. URL <https://journals.aps.org/pr/abstract/10.1103/PhysRevA.97.042315>.
- [7] Markus M. Breunig, Hans-Peter Kriegel, Raymond T. Ng, and Jörg Sander. LOF: Identifying Density-Based Local Outliers. *Proceedings of the 2000 ACM SIGMOD international conference on Management of data - SIGMOD '00*, pages 93–104, 2000. doi: 10.1145/342009.335388. URL <http://portal.acm.org/citation.cfm?doid=342009.335388>.
- [8] Kenji Yamanishi, Jun Ichi Takeuchi, Graham Williams, and Peter Milne. On-Line Unsupervised Outlier Detection Using Finite Mixtures with Discounting Learning Algorithms. *Data Mining and Knowledge Discovery 2004 8:3*, 8(3):275–300, 5 2004. ISSN 1573-756X. doi: 10.1023/B:DAMI.0000023676.72185.7C. URL <https://link.springer.com/article/10.1023/B:DAMI.0000023676.72185.7c>.
- [9] Ding Liu and Hui Li. Outlier Detection Using a Novel method: Quantum Clustering. 6 2020. URL <https://arxiv.org/abs/2006.04760v1>.
- [10] Fabio A. González, Alejandro Gallego, Santiago Toledo-Cortés, and Vladimir Vargas-Calderón. Learning with Density Matrices and Random Features. 2 2021. URL <https://arxiv.org/abs/2102.04394v4>.
- [11] Diego H. Useche, Andres Giraldo-Carvajal, Hernan M. Zuluaga-Bucheli, Jose A. Jaramillo-Villegas, and Fabio A. González. Quantum measurement classification with qudits. *Quantum Information Processing 2021 21:1*, 21(1):1–12, 12 2021. ISSN 1573-1332. doi: 10.1007/S11128-021-03363-Y. URL <https://link.springer.com/article/10.1007/s11128-021-03363-y>.
- [12] Michael A. Nielsen and Isaac L. Chuang. Quantum Computation and Quantum Information: 10th Anniversary Edition. *Quantum Computation and Quantum Information*, 12 2010. doi: 10.1017/CBO9780511976667.
- [13] Marcus Cramer, Martin B. Plenio, Steven T. Flammia, Rolando Somma, David Gross, Stephen D. Bartlett, Olivier Landon-Cardinal, David Poulin, and Yi Kai Liu. Efficient quantum state tomography. *Nature Communications 2010 1:1*, 1(1):1–7, 12 2010. ISSN 2041-1723. doi: 10.1038/ncomms1147. URL <https://www.nature.com/articles/ncomms1147>.

- [14] Daniel F.V. James, Paul G. Kwiat, William J. Munro, and Andrew G. White. On the measurement of qubits. *Asymptotic Theory of Quantum Statistical Inference: Selected Papers*, pages 509–538, 1 2005. ISSN 2469-9942. doi: 10.1142/9789812563071{_}0035.
- [15] Alberto Peruzzo, Jarrod McClean, Peter Shadbolt, Man Hong Yung, Xiao Qi Zhou, Peter J. Love, Alán Aspuru-Guzik, and Jeremy L. O’Brien. A variational eigenvalue solver on a photonic quantum processor. *Nature Communications* 2014 5:1, 5(1):1–7, 7 2014. ISSN 2041-1723. doi: 10.1038/ncomms5213. URL <https://www.nature.com/articles/ncomms5213>.
- [16] Yunchao Liu, Srinivasan Arunachalam, and Kristan Temme. A rigorous and robust quantum speed-up in supervised machine learning. *Nature Physics* 2021 17:9, 17 (9):1013–1017, 7 2021. ISSN 1745-2481. doi: 10.1038/s41567-021-01287-z. URL <https://www.nature.com/articles/s41567-021-01287-z>.
- [17] Ali Rahimi and Benjamin Recht. Random features for large-scale kernel machines. In *Advances in Neural Information Processing Systems 20 - Proceedings of the 2007 Conference*, 2009. ISBN 160560352X.
- [18] Fabio A. González, Vladimir Vargas-Calderón, and Herbert Vinck-Posada. Classification with quantum measurements. *Journal of the Physical Society of Japan*, 90(4):044002, 2021. doi: 10.7566/JPSJ.90.044002. URL <https://doi.org/10.7566/JPSJ.90.044002>.
- [19] Murray Rosenblatt. Remarks on Some Nonparametric Estimates of a Density Function. <https://doi.org/10.1214/aoms/1177728190>, 27(3):832–837, 9 1956. ISSN 0003-4851. doi: 10.1214/AOMS/1177728190.
- [20] Emanuel Parzen. On Estimation of a Probability Density Function and Mode. *The Annals of Mathematical Statistics*, 33(3):1065 – 1076, 1962. doi: 10.1214/aoms/1177704472. URL <https://doi.org/10.1214/aoms/1177704472>.
- [21] Raban Iten, Roger Colbeck, Ivan Kukuljan, Jonathan Home, and Matthias Christandl. Quantum circuits for isometries. *Phys. Rev. A*, 93:032318, Mar 2016. doi: 10.1103/PhysRevA.93.032318. URL <https://link.aps.org/doi/10.1103/PhysRevA.93.032318>.
- [22] Mikko Möttönen, Juha J. Vartiainen, Ville Bergholm, and Martti M. Salomaa. Transformation of quantum states using uniformly controlled rotations. *Quantum Info. Comput.*, 5(6):467–473, sep 2005. ISSN 1533-7146.
- [23] Bo Li, Yu Seung Kim, Rangachary Mukundan, al , Dusan Spornjak, Partha P Mukherjee, Jacob S Spendelow, John Davey, Lukasz Cincio, Yiğit Subaşı, Andrew T Sornborger, and Patrick J Coles. Learning the quantum algorithm for state overlap. *New Journal of Physics*, 20(11): 113022, 11 2018. ISSN 1367-2630. doi: 10.1088/1367-2630/AAE94A. URL <https://iopscience.iop.org/article/10.1088/1367-2630/aae94ahttps://iopscience.iop.org/article/10.1088/1367-2630/aae94a/meta>.

- [24] John Preskill. Quantum Computing in the NISQ era and beyond. *Quantum*, 2:79, 8 2018. ISSN 2521327X. doi: 10.22331/q-2018-08-06-79. URL <https://quantum-journal.org/papers/q-2018-08-06-79/>.